Relativistically Transparent Magnetic Filaments: Scaling Laws, Initial Results, and Prospects for Strong-Field Quantum Electrodynamics Studies

H. G. Rinderknecht,[1] T. Wang,[2] A. Laso Garcia,[3] G. Bruhaug,[1] M. S. Wei,[1] H. J. Quevedo,[4] T. Ditmire,[4] J. Williams,[5] A. Haid,[5] D. Doria,[6] K. M. Spohr,[6] T. Toncian,[3] and A. Arefiev[2]

[1]Laboratory for Laser Energetics, University of Rochester
[2]University of California, San Diego
[3]Helmholtz-Zentrum Dresden-Rossendorf, Germany
[4]University of Texas, Austin
[5]General Atomics, San Diego
[6]ELI-NP & IFIN-HH, Bucharest-Magurele, Romania

Relativistic electron motion and volumetric laser–plasma interaction at supercritical densities create a novel phenomenon: the relativistically transparent magnetic filament. A sufficiently intense laser in an overdense plasma induces a relativistic current filament that moves axially with the laser field. This current generates a quasi-static azimuthal magnetic field with strength comparable to the laser field. Surrounding the filament with a higher-density channel wall optically guides the laser pulse, allowing intense laser–plasma interaction over many Rayleigh lengths. This system operates as a relativistic plasma rectifier for laser light that efficiently converts the laser's electric and magnetic fields into a direct filamentary current and associated magnetic field. Electrons oscillate within the confining azimuthal magnetic field, facilitating direct energy gain from the laser and acceleration to hundreds of MeV. At the same time, the electron deflections within the magnetic field cause them to emit photons. Simulations predict that the azimuthal field strength reaches the megatesla level and the effective acceleration gradient exceeds 10^5 MeV/cm in the multipetawatt regime. The extreme magnetic-field strength and electron energy boost the radiated photon energy and the radiative power such that the magnetic filaments become efficient radiators of MeV photons.

We derived analytical scaling laws for the radiative properties of the magnetic filament phenomenon in terms of four parameters: the normalized laser amplitude $a_0 = |e| E/m\omega c$, a relativistic transparency parameter $S_\alpha \equiv n_e/n_e a_0$ with electron density n_e and critical plasma density n_c, the normalized laser focal radius $R_\lambda = (R/\lambda)$, and the normalized laser pulse duration $\tau_\nu = c\tau/\lambda$. To derive these laws, we made the following assumptions: First, the electrons are represented by a thermal distribution, with the number of accelerated electrons $N_e = n_e \pi R^2 c\tau$. Second, the characteristic temperature of the electron distribution scales linearly with time and can be represented as $T(t) = C_T a_0 mc^2 (ct/\lambda)$ for a constant of acceleration C_T. Third, the azimuthal magnetic field is produced by a relativistic, uniform current density as $B(r) = B_0 \pi(r/\lambda)S_\alpha$ for the laser's magnetic-field amplitude B_0. Fourth, the radiation power per electron is given by the synchrotron power spectrum and is evaluated using $B(r)$ at either the laser radius or a magnetic boundary $r_{mb} = \lambda f_i^{1/2} S_\alpha^{-1/2} \pi^{-1}$, which is a maximum radius that electrons can reach with a given initial momentum $\gamma_i \equiv f_i a_0$ for a constant f_i of order unity.[1] Fifth, the electrons radiate during a fraction of their orbit f_r. Lastly, the interaction ends by depletion of the laser pulse at a time $t_{cut} = f_t t_{max}$ for a constant factor f_t in the range $(0, 1)$ and t_{max} represents the time at which the energy in the electron population equals the initial laser energy. These assumptions result in scaling laws for photon energy $\langle \varepsilon^* \rangle$, total radiated energy $E_{\gamma,tot}$, number of photons N_γ, and efficiency η_γ as shown in Table I.

The scaling laws were compared to the results of 3-D particle-in-cell (PIC) simulations, as shown in Fig. 1. The PIC simulations used laser amplitude $a_0 = 190$ (intensity 5×10^{22} W/cm^2), $S_\alpha = 0.105$ ($n_e = 20 n_c$), $\tau = 35$ fs, and focal radius $R = 0.65$, 0.95, 1.35, 1.6, and 2.1 μm (Ref. 2). The acceleration constant C_T was inferred to have a value of approximately 0.08 from simulated

Table I: Scaling laws for relativistically transparent magnetic filaments.

Limit	$R < r_{mb}$	$R > r_{mb}$
$\langle \varepsilon_* \rangle / mc^2$	$\approx 1.4 \times 10^{-5} f_t a_0^2 R_\lambda \lambda_{\mu m}^{-1}$	$\approx 4.4 \times 10^{-7} f_i^{1/2} f_t^2 a_0^3 S_\alpha^{-3/2} \lambda_{\mu m}^{-1}$
$\dfrac{E_{\gamma,tot}}{mc^2}$	$\approx 7.7 \times 10^2 f_t^3 f_r C_T^{-1} a_0^5 R_\lambda^4 \tau_\nu$	$\approx 7.8 \times 10^1 f_i f_t^3 f_r C_T^{-1} a_0^5 S_\alpha^{-1} R_\lambda^2 \tau_\nu$
N_γ	$\approx 5.6 \times 10^8 f_t f_r C_T^{-1} a_0^2 S_\alpha R_\lambda^3 \tau_\nu \lambda_{\mu m}$	$\approx 1.8 \times 10^8 f_i^{1/2} f_t f_r C_T^{-1} a_0^2 S_\alpha^{1/2}$
η_γ	$\approx 2.9 \times 10^{-7} f_t^3 f_r C_T^{-1} a_0^3 R_\lambda^2 \lambda_{\mu m}^{-1}$	$\approx 2.9 \times 10^{-8} f_i f_t^3 f_r C_T^{-1} a_0^3 S_\alpha^{-1} \lambda_{\mu m}^{-1}$

E29602JR
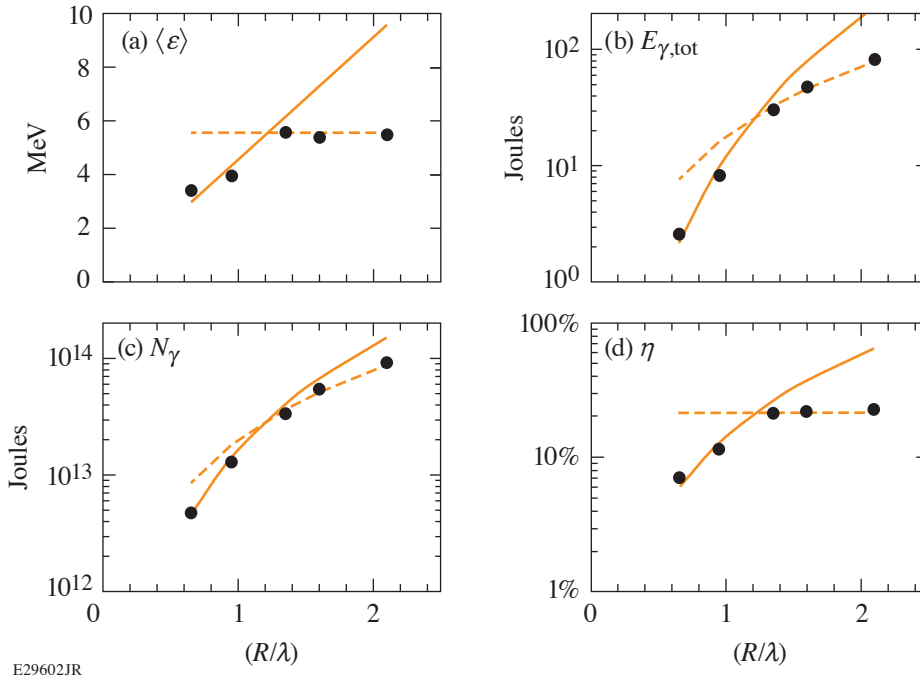
Figure 1

Comparison of derived scaling laws in the limit $R < r_{mb}$ (solid line) and $R > r_{mb}$ (dashed line) with 3-D PIC simulations in Ref. 2 (circles). (a) Characteristic photon energy, (b) total radiated energy, (c) total number of photons, and (d) radiation efficiency. Simulation results are for photons with energy above 1 MeV. Model coefficients are $f_i = 1.53$, $f_t = 0.31$, $f_r = 0.19$, and $C_T = 0.08$.

electron spectra; this value was used without loss of generality as the laws depend only on the composite constant (f_r / C_T). The scaling laws agree with the 3-D PIC simulations with reasonable values for the constants $f_i = 1.53$, $f_t = 0.31$, and $f_r = 19\%$.

Initial experiments were performed on the Texas Petawatt Laser to study this phenomenon. A peak intensity of 1.1×10^{21} W/cm^2 ($a_0 = 29.9$) was focused onto arrays of microchannels laser drilled in Kapton with a 6-μm inner diameter and filled with low-density CH foam with a density of 15 and 30 mg/cm^3 (5 and 10 n_c, respectively). Elevated electron temperatures were observed in two of eight shots with good laser–target alignment, in agreement with predictions from 3-D PIC simulations of laser–channel interaction, as shown in Fig. 2. This fraction is consistent with the likelihood of laser–channel interaction, given the
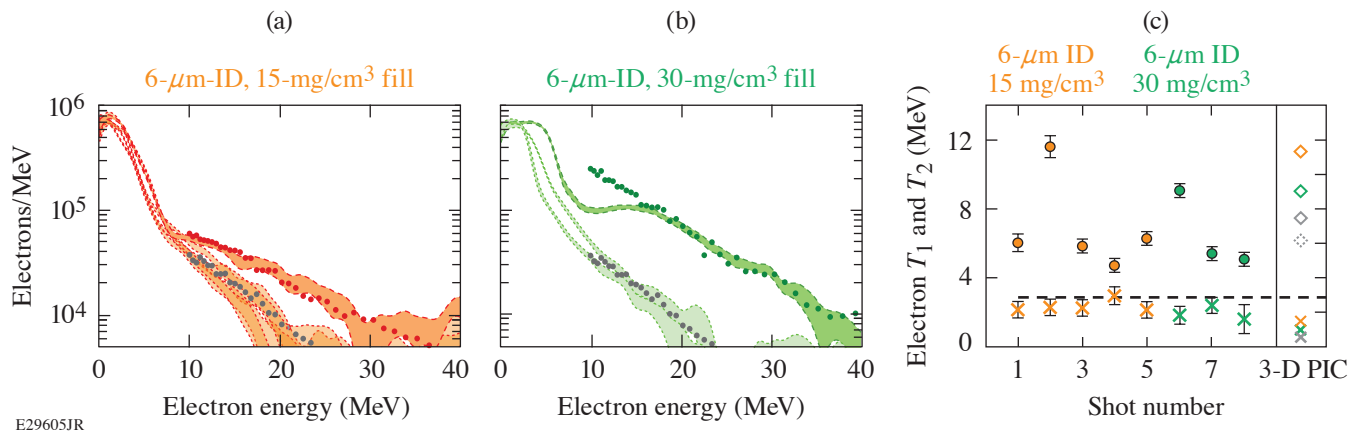
Figure 2

[(a),(b)] Electron spectra recorded on TPW experiments (curves) and from 3-D PIC simulations (circles). (c) Inferred electron temperatures on shots (circles) and from 3-D PIC simulations (diamonds). Channels with 5-n_c fill (orange), with 10-n_c fill (green), and planar 200-n_c target (gray).

pointing stability of 5-μm rms. We infer that the predicted magnetic filament phenomenon was observed in these experiments. The scaling laws will be used to design optimal targets for future experiments. At 10-PW laser facilities, efficiency approaching 50% is predicted for MeV photons.

1. Z. Gong *et al.*, Phys. Rev. E **102**, 013206 (2020).
2. T. Wang *et al.*, Phys. Rev. Applied **13**, 054024 (2020).